Sex-stratified single-cell RNA-Seq analysis identifies sex-specific and cell type-specific transcriptional responses in Alzheimer's disease across two brain regions.

Stella Belonwu
University of California San Francisco
Yaqiao Li
University of California, San Francisco
Daniel Bunis
University of California, San Francisco
Arjun Rao
University of California, San Francisco https://orcid.org/0000-0003-4480-3190
Caroline Warly Solsberg
UCSF https://orcid.org/0000-0001-7049-6281
Alice Tang
UCSF https://orcid.org/0000-0003-4745-0714
Gabriela Fragiadakis
University of California, San Francisco
Dena Dubal
University of California, San Francisco https://orcid.org/0000-0001-7504-4372
Tomiko Oskotsky
UCSF Bakar Computational Health Sciences Institute, University of California San Francisco, San Francisco, CA, USA https://orcid.org/0000-0001-7393-5120
Marina Sirota (Marina.Sirota@ucsf.edu)
UCSF Bakar Computational Health Sciences Institute, University of California San Francisco, San Francisco, CA, USA https://orcid.org/0000-0002-7246-6083

Article

Keywords: Alzheimer's disease, transcriptomic changes, sex differences

Posted Date: April 27th, 2021

DOI: https://doi.org/10.21203/rs.3.rs-418653/v1

Sex-stratified single-cell RNA-Seq analysis identifies sex-specific and cell type-specific transcriptional responses in Alzheimer's disease across two brain regions.

Stella A. Belonwu*[1,2], Yaqiao Li*[1,2], Daniel Bunis[1,3,4], Arjun Arkal Rao[3,4,5], Caroline Warly Solsberg[1,2], Alice Tang[1,6], Gabriela K. Fragiadakis[3,4,7], Dena B. Dubal[8,9,10], Tomiko Oskotsky[1,11], Marina Sirota[1,11]*

Affiliations:
[1]Bakar Computational Health Sciences Institute, University of California San Francisco, San Francisco, CA, USA
[2]Pharmaceutical Sciences and Pharmacogenomics Graduate Program, University of California San Francisco, San Francisco, CA, USA
[3]CoLabs, University of California, San Francisco, San Francisco, CA, USA
[4]Bakar ImmunoX Initiative, University of California, San Francisco, San Francisco, CA, USA
[5]Department of Pathology, University of California San Francisco, San Francisco, CA, USA
[6]Bioengineering Graduate Program, University of California San Francisco, San Francisco, CA, USA
[7]Department of Medicine, Division of Rheumatology, University of California, San Francisco, San Francisco, CA, USA
[8]Biomedical Sciences Graduate Program, University of California, San Francisco, San Francisco, CA, USA
[9]Neurosciences Graduate Program, University of California, San Francisco, San Francisco, CA, USA
[10]Department of Neurology and Weill Institute for Neurosciences, University of California, San Francisco, San Francisco, CA 94158, USA
[11]Department of Pediatrics, University of California San Francisco, San Francisco, CA, USA

*these authors contributed equally

Corresponding author: Marina Sirota, Associate Professor, UCSF Bakar Institute for Computational Health Sciences, 490 Illinois St, San Francisco, CA 94143 (marina.sirota@ucsf.edu)

Abstract

Alzheimer's disease (AD) is a pervasive neurodegenerative disorder that disproportionately affects women. Since neural anatomy and disease pathophysiology differ by sex, investigating sex-specific mechanisms in AD pathophysiology can inform new therapeutic approaches for both sexes. Here, we utilized nearly 74,000 cells from human prefrontal and entorhinal cortex samples from the first two publicly available single-cell RNA sequencing AD datasets to study cell type-specific sex-stratified transcriptomic perturbations in AD. Our examination at the single-cell level revealed that sex-specific gene and pathway differences in AD were most prominently observed in glial cells of the prefrontal cortex. In the entorhinal cortex, we observed the same genes and pathways to be perturbed in opposing directions between sexes in AD relative to healthy state. Our findings contribute to growing evidence of sex differences in AD-related transcriptomic changes, which can fuel the development of therapies that may prove more effective at reversing AD pathophysiology.

Introduction

Alzheimer's disease (AD) is an irreversible neurodegenerative disorder that causes progressive memory decline, cognitive deficits, and behavioral changes[1–3]. It is the most common form of dementia and is reaching epidemic proportion as a result of extended life expectancies and increased elderly populations worldwide[4,5]. It is of high priority to find disease-modifying treatments for AD, as more than five million people are diagnosed with AD currently in the United States, a number estimated to triple by 2050[6,7].

Although first described more than a century ago[8], the underlying molecular mechanisms of AD remain elusive[9]. Extensive research efforts reveal that AD is histologically characterized by pathological brain aggregates including extracellular amyloid-β (Aβ) plaques, and intracellular tau protein neurofibrillary tangles (NFTs)[10,11]. Increasing evidence suggests that neuroinflammation and brain dysfunction led by neuronal supporting cells, which include microglia, astrocytes, and oligodendrocytes, could contribute to AD pathophysiology[12,13]. These pathological features are accompanied by impaired neurotransmitter signaling, dysregulated neuronal metabolism, neuronal loss, and cerebral atrophy[14–16]. Overall, the exact pathogenesis of AD remains uncertain, which hinders the development of effective therapies.

Sex differences have been clinically documented in AD[17,18], yet the underlying cause for these differences are not well understood. Approximately two thirds of AD diagnoses are in women[19]. In addition to greater longevity in females[20], other biological differences may be responsible for the higher prevalence and accelerated cognitive decline observed in women during disease progression[18,21,22]. For instance, a longitudinal study examining a postmortem cohort of about 1,500 individuals observed that in the presence of similarly high Aβ burden, females exhibited faster cognitive decline than males[22], suggesting females might be more susceptible to Aβ

toxicity. Furthermore, after adjusting for age and education, women had a higher tau tangle density[22,23]. Among genetic risk factors implicated in AD, the apolipoprotein E (*APOE*) ε4 risk allele has been observed to have a differential influence and increased risk for AD in women compared to men[24,25]. Sex hormones, especially the decline in hormone levels post-menopause, could also contribute to sex differences in AD progression. For example, after menopause, women experience an abrupt loss of progesterone[26], which was previously shown to be neuroprotective by promoting myelin repair and reducing inflammation[27,28]. In fact, compared to men, women experience more inflammation-driven symptoms and have an increased risk for autoimmune diseases[29–31]. These findings suggest that investigating sex differences in AD will not only provide insight into deciphering the fundamental biological and mechanistic causes of AD pathogenesis, but also highlight the necessity of developing personalized therapeutic strategies.

Previous studies suggest that cellular and molecular heterogeneity in AD pathogenesis[32,33] and brain immune cell dysfunction contribute to sex-specific AD pathophysiology[34]; however, sex-specific disease complexity at single-cell resolution is masked in bulk brain sequencing analysis. Recent advances in single-cell RNA sequencing technology and the increasing availability of human transcriptomic datasets present a novel opportunity to examine cell type-specific transcriptional alterations in AD brain pathology. In recent years, two single-nucleus RNA-Seq (snRNA-Seq) datasets were generated from the prefrontal[35] and entorhinal[36] cortices of age and sex-matched human AD patients and cognitively normal controls. For the prefrontal cortex dataset, Mathys and colleagues performed differential expression analysis on transcriptomic results of 80,660 droplet-based nuclei within six major cell types across 48 individuals of varying degrees of AD pathology. They identified cell type-specific differentially expressed genes (DEGs) in AD in comparison to control individuals and sex-specific cell subpopulations associated with AD pathology. While the authors reported on the general sexual dimorphic

transcriptional response to AD pathology, they did not extensively examine sex-specific DEGs in the individual brain cell types or delineate any subsequent sex-specific molecular pathway enrichments in AD. Similar to the Mathys analysis, Grubman and colleagues analyzed 13,214 droplet-based nuclei with postmortem tissue from the entorhinal cortex of 12 age and sex-matched human AD patients and controls. Besides investigating the likelihood of sex as a covariate factor for DEG variance observed, no sex difference analysis was performed in this study.

Understanding gene expression changes unique to each sex provides opportunities to decipher molecular underpinnings that differentially contribute to AD in males and females. In this study, we leveraged the two snRNA-Seq datasets to characterize sex-stratified cell type-specific gene expression perturbations in AD and to identify sex-specific disease-associated cellular pathways as potential precision therapeutic targets. In both brain regions, we identified sex-specific disease changes primarily in glial cells and observed samples to cluster by sex when examining gene expression changes in AD compared to controls. Our findings will be of fervent interest to the field in studying differing vulnerabilities between sexes in AD.

Results

Sample classification and analytic workflow

Samples were categorized into cases and controls based on tau tangle and Aβ plaque burdens, using Braak clinical staging and Consortium to Establish a Registry for Alzheimer's Disease (CERAD) scores[37], respectively (AD: Braak stage ≥ IV, CERAD score ≤ 2; Control: Braak stage I-III, CERAD score ≥ 3). This resulted in single-nucleus RNA-Seq datasets containing 17,723 genes expressed by 62,741 cells from the prefrontal cortex, and 10,846 genes expressed by 11,284 cells from the entorhinal cortex, which were acquired from different sets of individuals (Figure 1). In both brain regions, a sex-stratified differential gene expression (DGE) analysis was performed comparing AD cases to controls, with *APOE* genotype as a covariate, in astrocytes (Ast), microglia (Mic), excitatory neurons (Ex), inhibitory neurons (In), undifferentiated neurons (Neu), oligodendrocytes (Oli), and oligodendrocyte progenitor cells (OPCs) (Supplementary Tables 1 and 2). For the entorhinal cortex cohort, data integration was performed and *APOE* genotype was included as a covariate in our DGE analysis to account for batch effects and avoid collinearity in our model. Differentially expressed genes (DEGs) were determined using a Benjamini-Hochberg adjusted p-value < 0.05 and absolute log2 fold change (LFC) > 0.25 as cutoffs. DEGs were passed as inputs for pathway enrichment analysis, which provided pathways to be used as inputs for subsequent network analysis. We examined gene expression and pathway network differences in AD versus neurotypical cells to identify cell type- and brain region- specific and non-specific differences based on sex.

DGE analysis in the prefrontal cortex reveals modest sex-specific disease related changes specifically in glial cell types

Leveraging data from Mathys et al., from our sex-stratified DGE analysis, we identified DEGs meeting significance and LFC thresholds (Table 3) in all cell types except male inhibitory

neurons when comparing AD to non-AD (Supplementary Table 3). We identified 73 DEGs across all cell types in the prefrontal cortex (Table 3, Supplementary Table 3). Of these DEGs, 36 were shared in both sexes, while 8 and 29 were specific to AD compared to control males and females, respectively. We also observed more shared DEGs in AD case versus control female signatures versus male signatures across the cell types (Fig. 2a), which is consistent with previous bulk tissue analysis[34]. Some of the differentially expressed genes include *LINGO1*, a negative regulator of myelination[38,39], which we found upregulated in all AD compared to control female cell types; *SLC1A3*, which encodes excitatory amino acid transporter 1 that transports glutamate in the synaptic cleft[40] and was perturbed in all female AD compared to control cell types except oligodendrocytes and OPCs; and *SPP1*, a protein involved in neuroinflammation also known as Osteopontin[41] that we observed to be upregulated in AD versus control samples of both female and male excitatory neurons and microglia, as well as female astrocytes and inhibitory neurons. Also, clustering samples by AD compared to control pseudo-bulk cell type gene expression (Fig. 2b) showed samples to be clustered primarily by sex before cell type identity for all cell types except excitatory neurons.

In addition to identifying shared DEGs across cell types and sexes, we also observed a larger range of LFC in the analysis of female AD versus control ([-0.423, 1.058], median=0.314) compared to the analysis of male AD versus control ([-0.370, 0.620], median=0.343). Within each cell type, we observed DEGs, a number of which are relevant to and have been studied in AD (e.g. *NRXN1*[42], *SPP1*[41], *DHFR*[43], *SGK1*[44], *ERBB2IP*[45]), meeting significance and LFC thresholds. These DEGs are shared by both sexes in AD versus control astrocytes, microglia, and excitatory neurons, with consistent directionality in both sexes (Fig. 2c; Fig. 2d, yellow color; Supplementary Figure 3). Overall, in the prefrontal cortex, we identified more disease-related transcriptomic changes in females and differences in gene expression primarily among glial cells.

DGE analysis in the entorhinal cortex reveals greater transcriptomic changes in male disease, and opposite transcriptomic changes between sexes

Leveraging data from Grubman et al, we identified DEGs (Table 4) in all cell types stratified by sex, when comparing AD to non-AD (Supplementary Table 4). We identified 232 DEGs across all cell types in the entorhinal cortex (Table 4, Supplementary Table 4). Of these DEGs, 211 were shared in both sexes, while 20 and 1 were specific to AD compared to control males and females, respectively. We observed shared DEGs across cell types when comparing AD versus control samples in both sexes (Fig. 3a). Some of these globally shared genes include *CLU*[9,46], *HSPA1A*[47], *RBFOX1*[48], and *CST3*[49]**,** which are relevant in AD progression. Clustering of samples by AD compared to control pseudo-bulk cell type-specific gene expression (Fig. 3b) showed samples to cluster by sex before cell type identity for every cell type and highlighted opposing gene expression patterns based on sex. Indeed, interestingly, 186 of the 211 DEGs shared between male and female AD were regulated in opposite directions with respect to controls, at least in some cell types.

When comparing the magnitude of gene expression changes across sexes in AD versus control samples, we found males to have a greater range of LFCs ([-2.174, 3.461], median=0.567) compared to females ([-1.657, 2.649], median= -0.436). We visualized these differences in DEGs such as *LINGO1,* which had a higher fold change difference in male astrocytes (3.415) compared to female astrocytes (0.4); *GPM6A*, which was upregulated in male oligodendrocytes and downregulated in female oligodendrocytes; *CST3*, which was upregulated in male neurons, male oligodendrocytes, and male and female OPCs, and downregulated in female neurons, female oligodendrocytes, and male and female astrocytes; and *LINC00486*, which was upregulated in all cell types of both sexes with an average LFC in males of 1.9 compared to 1.0 in females **(**Fig. 3c). Generally, directly comparing AD vs control DEGs within each cell type, we not only observe a subset of genes with directionally consistent changes among males and

females (Fig. 3d, yellow color; Supplementary Figure 3), but we also observed numerous changes in opposing directions across sexes (Fig. 3d, pink color; Supplementary Figure 3), and a higher magnitude of disease-related changes in males compared to females.

Comparative analysis across brain regions reveals more shared transcriptomic sex differences in the entorhinal cortex

We compared DEG results from the prefrontal and entorhinal cortices to determine whether changes in each sex were consistent across brain regions. Overall, we observed more overlaps in across sex DEGs to be in the entorhinal cortex (Fig. 4a). Additionally, clustering samples by AD compared to control pseudo-bulk cell type gene expression (Fig. 4b) showed samples to be clustered primarily by brain region and sex, and not by cell type.

Pathway and network analysis reveals sex-specific transcriptomic perturbations in glial cells in the prefrontal cortex and sex-shared, but flipped AD-enriched pathways in the entorhinal cortex

Beyond identifying sex-dimorphic disease-associated genes, we performed a gene set enrichment analysis to elucidate potential biological mechanisms implicated in disease progression that are either shared or unique to each sex and to reveal the interconnections between disease-linked pathways within AD. The pathway enrichment was performed in g:Profiler[50], a web tool that performs functional enrichment analysis from a given gene list, using separate lists of upregulated and downregulated DEGs with an adjusted p-value <0.05 and relaxed absolute LFC above 0.1 in cell types of each sex as inputs. Significantly enriched biological pathways with an adjusted p-value < 0.05 were applied to EnrichmentMap[51], a functional category grouping method from the Cytoscape software, to identify pathway network clusters annotated by associated biological processes (Fig. 5, Supplementary Figures 3 and 4).

Female and male AD compared to control excitatory neurons of the prefrontal cortex shared six common enriched clusters of pathways (Fig. 5a), which were all perturbed in the same direction for both sexes. Two of these clusters (neurotransmitter glutamate/aspartate transmembrane activity and carboxylic acid biosynthetic process) were upregulated in disease in both sexes. Of the four downregulated pathway clusters, three were related to synaptic activity (modulation of the synaptic membrane, neurotransmitter release, and synapse assembly/cell junction organization), indicating a dysregulation of synaptic plasticity in AD excitatory neurons. The other downregulated pathway cluster was plasma membrane morphogenesis, which consisted of pathways including axonogenesis, cellular projection, and plasma membrane organization. (Supplementary Tables 5 and 6).

In prefrontal cortex excitatory neurons, we also identified uniquely enriched disease pathway clusters for each sex (Fig. 5a). Female excitatory neurons showed upregulation of the HOXA5 factor, a DNA-binding transcription factor that regulates cell morphogenesis and tumor suppressor that inhibits proliferation and induces apoptosis[52], and downregulation of inflammatory-mediated cell to cell interaction through adhesion and molecule binding. Interestingly, a recent epigenome-wide association study examining samples in the prefrontal cortex and superior temporal gyrus observed elevated DNA methylation of the *HOXA* gene cluster to be associated with neuropathology in AD[53]. In male excitatory neurons, we observed upregulation of axon regeneration, and downregulation of distal axonal growth cone polarization. Interestingly, we also observed downregulation of tetrahydrobiopterin (BH4) synthesis, which is important for the production of essential neurotransmitters[54], and Rho GTPase activities in male AD compared to control excitatory neurons. Overall, excitatory neurons of the prefrontal cortex shared most case vs control differentially enriched pathways between male and females, the majority of which were downregulated in AD.

Similar to enriched pathways in disease observed in excitatory neurons, the inhibitory neurons of the prefrontal cortex showed upregulation for glutamate/aspartate activities in both female and male AD inhibitory neurons compared to controls (Fig. 5b). Like male AD excitatory neurons, male AD inhibitory neurons also showed downregulation of axonal growth cone polarization and BH4 activities compared to controls. In addition, males specifically demonstrated upregulation in anterograde synaptic transmission and downregulation of nitric synthase, heat shock protein 90 (HSP90) complex, voltage potassium transporter, and kainite calcium-permeable receptors activities in AD. The *ITGAV-ITGB-SPP1* complex, with known function in cell adhesion[55] and without previous links to AD, was uniquely upregulated in male inhibitory neurons. Of note, the pathway cluster neuronal projection was upregulated in females and downregulated in males, consistent with the enriched upregulated pathways clusters uniquely observed in females, which were modulation of spine morphogenesis and synaptic membranes. Lastly, the transcription factors, nuclear receptor TLX (essential for the regulation of self-renewal, neurogenesis and maintenance in neuron stem cell)[56] and nuclear protein HOXB2 (involved in cellular development)[57], were upregulated only in AD female inhibitory neurons.

Unlike in neurons in the prefrontal cortex, we identified a variety of commonly enriched disease pathway networks in entorhinal cortex neurons that were regulated in opposite directions for the sexes (Fig. 5c). For instance, amyloid-beta binding/fibril formation, mitochondrial abnormality, coupled electron ATP metabolic process, demyelination/remyelination, cellular metabolism, extracellular organelle exosome vesicle and cation transmembrane transport were among the clusters downregulated in females and upregulated in males. We did not observe any pathway networks unique to female neurons; however, for the AD male neurons in the entorhinal cortex, we identified pathways in maintaining cellular metabolism and homeostasis, through the upregulation of genes involved in axon myelination, regulation of the metabolic process, cell

component locomotion, cytoskeleton organization, and intracellular ferritin complex (iron storage). In male neurons, we also observed synaptic activity deficiency, indicated by the downregulation of pathways in synaptic vesicle transport, presynaptic assembly at cell junction, synaptic membrane clustering, postsynaptic membrane morphogenesis, chemical regulation at the synapse, neuroligin family protein binding, and ionotropic receptor signaling. Additionally, male AD neurons compared to controls also showed downregulation in plasma membrane regulation, cell projection, and developmental process in differentiation. As a whole, while sex differences are minimal in the neurons of the prefrontal cortex, we observed overwhelmingly shared but inversely regulated enrichment pathways in the neurons of the entorhinal cortex.

Microglia, the resident immune cells of the brain, have gained growing recognition as being critically involved in AD pathogenesis due to their key role contributing to neuroinflammation, a prominent feature of AD[58]. Only a few significantly enriched disease pathways were observed in microglial cells of the prefrontal cortex and none were shared across sexes (Fig. 5d). We observed upregulation of axon sprouting in response to injury in males, as well as an enriched upregulated pathway in axonogenesis regulation in females (Supplementary Table 6). Interestingly, a cluster of the PDE4B-DISC1-complex, with important functions in cAMP-regulated signal transduction and synaptic plasticity,[59] was downregulated in females. The phosphodiesterase 4B (PDE4B) enzyme was previously shown to be pro-inflammatory in microglia and is currently under study as a therapeutic target for neuroinflammation and cognitive function impairment[59].

Microglia in the entorhinal cortex had mostly downregulated pathway clusters in females and upregulated pathway clusters in males (Fig. 5e). Amyloid fibril formation, chaperone-mediated autophagy, protein folding, protein stability regulation, cell junction synapse, neurogenesis structure development, and cell body assembly were among the clusters shared by both sexes

but downregulated in females and upregulated in males. Protein homeostasis was altered in disease for females, as shown by downregulation of tau protein kinase activity, tau protein binding, protein folding chaperone, and histone deacetylase binding. Protein degradation and secretion were also downregulated in females with AD compared to controls, as indicated through downregulation of lytic vacuole lysosome and secretory granule vesicle exocytosis respectively. Interestingly, nitric oxide synthase 3 (NOS3), which is involved in a complex cascade of events in oxidative stress that may induce cellular injury and accelerate neurodegenerative changes[60], and its chaperone, HSP90[61], were downregulated in AD females compared to controls. In males, myelination in axon ensheathment, synaptic signaling transmission, and energy coupled proton transport were upregulated. We also identified downregulation of two microRNA clusters, hsa-miR-190a and hsa-miR-3605, in AD males compared to healthy controls. These are potentially important findings because epigenetic modulation by microRNAs has the capacity to modify microglial behavior in physiological conditions, and dysregulation of microRNAs could mediate microglial hyper-activation and persistent neuroinflammation in neurological diseases[62]. Overall, we observed extensive sex-specific pathway enrichments in microglial populations of AD compared to controls for both brain regions, but especially pronounced in entorhinal cortex.

Furthermore, astrocytes, oligodendrocytes, and OPCs also demonstrated sex-specific pathway perturbations in both prefrontal and entorhinal cortices (Supplementary Fig. 3 and 4). In astrocytes, which normally function to maintain overall brain homeostasis, we observed downregulated plasma and presynaptic membrane components and upregulated postsynaptic asymmetric synapse density in the prefrontal cortex of AD compared to controls in both sexes. In female AD astrocytes, we observed downregulation in pathways related to amino acid transport and vascular transport across the blood brain barrier. Although the downregulation of these pathways was not observed in males, a related pathway cluster, presynaptic filopodia

activities, was downregulated. These observed pathway networks suggest that the same biological process, regulation of synaptic activities, was disrupted in both sexes but via different mechanisms.

In oligodendrocytes, which provide support and insulation to axons in the brain, we observed downregulation in pathways related to regulation of synaptic activity in both female and male AD compared to controls, indicated by the downregulated clusters of cleft regulation, presynaptic assembly, and transmembrane transport channel in females, and neurotransmitter secretion, transmembrane ion transporter, and postsynaptic membrane potential regulation in males. Interestingly, pathways related to cell morphological changes and energy production were upregulated in males and downregulated in females, such as pathway clusters of neuron projection organization, cell migration/locomotion, cellular component organization, ATP coupled electron transport, mitochondrial NADH dehydrogenase, suggesting oligodendrocyte responses were sex-specific when challenged by disease.

Lastly, we observed upregulation of membrane morphogenesis in female OPCs in the prefrontal cortex, as well as related pathway cluster, *TROY-NGR-LINGO1-NGFR* complex, which plays essential roles in the inhibition of axonal regeneration[63]. In the entorhinal cortex, a few pathways were downregulated in female and male OPCs, including cell junction synapse assembly, glutamatergic synapse, and plasma membrane intrinsic component. The male OPCs of the entorhinal cortex were overwhelmingly enriched with upregulation in neuronal development, axon ensheathment, neuron myelination, metabolic protein regulation, as well as ion and vesicle transport, with the exception that synaptic membrane adhesion molecules were downregulated. Although inconclusive due to the unbalanced numbers of significantly enriched pathways obtained in OPCs from both sexes, our observations suggest that AD female OPCs in the

prefrontal cortex diverge more from controls compared to male OPCs, whereas in the entorhinal cortex, AD male OPCs were more perturbed by disease status compared to females.

Discussion

Men and women show differing vulnerabilities to AD, with increased longevity and prevalence in women, and decreased tau and possibly cognitive decline in men[17–19,21,22]. To understand how AD presents in each sex on a cell type-specific level, we performed a sex-stratified differential gene expression (DGE) and pathway network analysis on the five main brain cell types using the first two publicly available human single nucleus RNA-Seq datasets. The two datasets target two separate brain regions, the entorhinal and prefrontal cortices, and we analyzed each in a sex-stratified manner, then compared findings across sexes and brain regions to highlight both general and cell type-, region-, and sex- specific transcriptional phenotypes of AD (Fig. 1).

Our gene level analysis in the prefrontal cortex showed more disease-related changes in females with AD than in males in comparison to their respective control cohorts (Fig. 2). There were also more DEGs shared among cell types in females versus males (e.g. *LINGO1*[38,39], *SLC1A3*[40], *SPP1*[41]). While we observed a larger range of fold change in our female DGE analysis, an overall comparison across sex within each cell type showed modest differences in disease related gene expression changes. Additionally, through clustering prefrontal cortex samples based on AD compared to control pseudo-bulk gene expression, we observed samples to cluster first by sex in all cell types except excitatory neurons. In the entorhinal cortex however, we observed a higher magnitude of change in males with AD than in females in comparison to their respective control cohorts. Compared to the prefrontal cortex, we observed more overall DEGs and many global changes across cell types (Fig. 3a). Through clustering entorhinal cortex samples by AD compared to control pseudo-bulk gene expression, we observed samples to cluster by sex for all cell types, and also observed opposing expression patterns across sex (Fig. 3b), which we visualized in a handful of DEGs and examined in a pairwise manner (Fig. 3c-d). Moreover, our comparative analysis across brain regions showed

more DEG overlaps across sex in the entorhinal cortex, of which we observed flipped directionality in disease related gene expression changes (Fig. 3, Fig. 4).

From the gene-set enrichment and pathway clustering network analysis, we identified sex-specific pathway network changes, which are potentially involved in AD pathogenesis through mechanisms unique to each sex (Fig. 5, Supplementary Figure 3 and Supplementary Figure 4). Our results demonstrated that diseased neurons in the prefrontal cortex shared more enriched pathways compared to glial cells in both sexes, indicated by the proportion and directionality of the shared pathways. This may suggest that neuronal pathophysiology is similar in female versus male, and glial pathophysiological changes are more distinctive in contributing to sex-specific disease progression in AD. Despite neurons being more similar than glial cells, interesting sex-specific biological perturbations were revealed in neurons of females and males separately. Diseased female neurons showed increased activation in cell membrane morphogenesis but reduction in the production of tight junction complexes. A few transcriptional factors were uniquely upregulated in females, such as HOXA5, HOXB2, and TLX. Future studies investigating the role of overactivation of these genes in AD, especially in females, could lead to better mechanistic understanding of AD pathogenesis and potential therapies targeting these transcriptional factors in females. In diseased male neurons, nitric oxide synthase (NOS) activity was downregulated, as well as its regulating factors, the HSP90 complex and co-factor BH4. BH4 has been extensively studied in its role of regulating nitric oxide production from nitric oxide synthases and superoxide anion radical (O_2^{*-}) release in the endothelium[64]. Our pathway enrichment analysis suggests that perhaps excessive O_2^{*-} in diseased male neurons due to dysregulated NOS activities and BH4 levels could lead to neuronal stress and death. Therefore, resolving the chronic BH4 deficiency and change in redox state of neurons pharmacologically could be a beneficial therapy for AD male patients.

The glial cells in the prefrontal cortex shared just a few enriched pathways, out of hundreds detected collectively, between AD males and females: nine in astrocytes (Supplementary Figure 3a), two in oligodendrocytes (Supplementary Figure 4a), and none in microglia and OPCs (Fig. 5d and Supplementary Figure 4c) (these numbers do not include shared pathways regulated in opposite directions in female vs male). Besides downregulation of membrane morphogenesis, both female and male diseased astrocytes demonstrated decreased synaptic regulation, but different pathways for different components were involved. In females, we observed a decrease in glutamate transmembrane transport, vascular transport, and organic acid symporter activities. In males, we observed a decrease in presynaptic intrinsic component filopodia activities. These pathways were interconnected, indicating that they belong to related biological processes, which suggests that similar resulting synaptic deficiencies were observed in both sexes but resulted from different pathway mechanisms. These are compelling evidence for focusing on glial cell pathophysiological changes in studying sex-difference in AD pathogenesis.

In the entorhinal cortex, while similar to in the prefrontal cortex, we identified sex-specific perturbed pathway networks in all cell types, where the pathways shared across sexes were overwhelmingly of opposite direction, with most pathways downregulated in female and upregulated in males (Fig. 5, Supplementary Figure 3 and Supplementary Figure 4). Out of the five cell types investigated, two were dominated by enriched pathways detected in males (neurons and OPCs), one was dominated by enriched pathways detected in females (oligodendrocytes), and two were more evenly distributed (microglia and astrocytes). The diseased female microglia demonstrated deficiency in tau protein processing uniquely, by downregulation of tau kinase activity and tau protein binding. Additionally, disruption of cellular protein homeostasis was also observed in female microglia, indicated by downregulation of protein folding chaperone, histone deacetylase binding, lysosomal activity, and exocytosis vesicle secretion. The female microglia were perceived as deficient in dealing with the

degradation of the debris and cellular waste that they phagocytosed while the male microglia were active at combating the disease environment by upregulating axonal myelination, synaptic transmission signaling, cellular component assembly and energy production through energy coupled proton transport. As immune cells are critical for repair after injury, this may indicate that female AD risk relates to decreased ability to properly recover after deleterious events over time.

While we observed evidence of sex-dimorphic disease changes in glial cells in AD, it is important to note some limitations in the study. First, the data sets were limited in sample size. The entorhinal cohort consisted of six cases (two female, four male) and five controls (two female, three male) (Fig. 1, Table 2), while the prefrontal cohort consisted of 20 cases (10 female, 10 male) and 22 controls (10 female, 12 male) (Fig. 1, Table 1). Second, there were batch effects in the entorhinal cortex data introduced by the study design. This was overcome by performing data integration and including *APOE* genotype as a covariate in our DGE analysis to account for batch and avoid collinearity in our model. Next, literal biological sex could be a misleading classifier for trans* individuals. A properly powered study of differences between male versus female versus recipients of testosterone- versus estrogen-focused hormone replacement therapy might help narrow down a genetic versus hormonal basis of DEGs deemed sexually dimorphic. Finally, although both datasets were age-matched, they were not *APOE* genotype matched. APOE4 is the largest risk factor in AD, and as a result, we would expect some transcriptional differences based on the *APOE* genotype of a sample[66]. In the prefrontal cortex cohort, female samples had cases but not controls with the ε4 allele of *APOE*, and male samples had cases and only one control sample with ε4 allele of *APOE* (Table1). In the entorhinal cortex cohort, female samples included one of two cases and no controls with an ε4 allele of *APOE*, and all male cases had at least one ε4 allele of *APOE*, and one of three control samples had an ε4 allele of *APOE* (Table 2). While we accounted for *APOE* genotype as

a covariate in the DGE analysis, the interactions of sex and *APOE* genotype may still explain trends that we observe. We hope that future explorations of sex-specific transcriptomic changes in AD will include larger datasets from more brain regions with individuals of diverse age groups, racial and ethnic backgrounds, and *APOE* genotypes.

In general, our findings suggest that AD signatures in neurons in the prefrontal cortex were more similar in females and males compared to glial cells, as indicated by the proportions of sex-shared genes and pathways with directionally similar regulation in each cell type (Fig. 5, Supplementary Figure 3 and Supplementary Figure 4). In the entorhinal cortex, while we identified sex-specific perturbed pathways in each cell type, the sex-shared pathways were overwhelmingly opposite in the direction of regulation, with most pathways downregulated in female and upregulated in males or conversely regulated for a few other pathways. Sex-stratified findings in the entorhinal cortex could relate to recent observations that women show more tau deposition early on in the AD trajectory, specifically in this area[67]. Perhaps future studies could also explore the specific association between the gene changes in the entorhinal region with tau burden. Collectively, these observed sex-specific transcriptomic changes provide a valuable resource to study sex-specific cell type-specific pathophysiology of AD. Although expression differences in all cell types may be relevant to disease mechanisms in AD, we focused on discussing the cell types with the most compelling findings in our study: neurons, astrocytes and microglia. We hope this work serves as a resource for follow-up studies that will examine more deeply all the cell types and their specific roles leading to sex-specific AD pathophysiology.

Methods

Materials Availability

This study did not generate new unique reagents.

Data and Code Availability

We accessed single nuclei RNA-Seq counts data from the prefrontal cortex via the Accelerating Medicines Partnership Alzheimer's Disease Project (AMP-AD) Knowledge Portal under the Religious Orders Study and Memory and Aging Project (ROSMAP) (https://www.synapse.org/#!Synapse:syn18485175; https://www.synapse.org/#!Synapse:syn3157322), and from the entorhinal cortex via a data repository provided by Grubman et al. (http://adsn.ddnetbio.com/). The entorhinal cortex dataset and supporting materials may also be accessed via the Gene Expression Omnibus (GEO) under the accession number GSE138852. Access to the prefrontal cortex dataset requires a formal request to ROSMAP. All code necessary for recreating the reported analyses and figures within R are available at: https://github.com/stebel5/AD_SexDiff_snRNAseq.

Study Cohorts

The prefrontal cortex cohort comprised age and sex matched samples from 24 males and 24 females with varying degrees of AD pathology. We reclassified samples based on tau and amyloid β (Aβ) plaque burden, using Braak clinical staging and Consortium to Establish a Registry for Alzheimer's Disease (CERAD) scores, respectively. We defined cases as individuals with severe tau deposition (Braak ≥ IV), and high Aβ load (CERAD ≤ 2), and non-AD controls as individuals with low tau (Braak ≤ III) and low Aβ load (CERAD ≥ 3). For our sex-stratified analysis, we focused on 20 cases (10 female, 10 male) and 22 controls (10 female, 12 male) (Fig. 1, Table 1).

The entorhinal cortex cohort consisted of age matched 6 (2 female, 4 male) AD patients and 6 (2 female, 4 male) control subjects, which were classified based on pathological analysis of amyloid β plaques, Braak clinical staging, and cognitive impairment records as done in the prefrontal cohort. Note, all cases in this cohort have numerous diffuse and neuritic amyloid beta plaques, and a Braak staging score of VI. We excluded one control male sample with the APOE2/4 genotype. For our sex-stratified analysis, we focused on 6 cases (2 female, 4 male) and 5 controls (2 female, 3 male) (Fig. 1, Table 2).

Single Cell Data Processing, Cell Type Identification and Batch Correction

Data processing and analysis was performed separately for each dataset with R[68] version 4.0.0 (2020-04-24) via RStudio[69], using Seurat[65] (v3.1.5). Visualizations were created with BioRender (https://biorender.com/) (Fig. 1), dittoSeq (v1.0.2) (https://github.com/dtm2451/dittoSeq/), a package for analysis and visualization of bulk and single-cell transcriptomic data in a color blind friendly manner, ggplot2[70], and UpsetR[71].

Prefrontal Cortex

Seurat's Read10X function was used to generate a count data matrix using the filtered count matrix of 17,296 genes and 70,634 cells, gene names, and barcodes files provided by 10X. A Seurat object was created with the count data matrix and metadata and filtered to keep genes present in at least 3 cells, and cells meeting cohort selection criteria of at least 200 genes. Log normalization was performed using Seurat's NormalizeData function with a scale factor of 10,000, and highly variable features were identified using Seurat's FindVariableFeatures, returning 3,188 features, as specified in the original paper. The data matrix was then scaled using Seurat's ScaleData function with *nCount_RNA* regressed out, and dimensionality reduction through Uniform Manifold Approximation and Projection (UMAP) was performed with the appropriate dimensions selected based on the corresponding principal component analysis

(PCA) elbow plot. UMAP plots confirmed that there were no confounding variables (Supplementary Figure 1).

To identify cell types, following similar steps as Grubman and colleagues[36], we applied Seurat's AddModuleScore function to lists of 200 brain cell type markers from the BRETIGEA[72] package to identify each cell type. Cell types assessed included astrocytes, neurons, microglia, oligodendrocytes, oligodendrocyte progenitor cells, pericytes, and endothelial cells. Cells with the highest score across brain cell type markers were labeled the corresponding cell type, and if the highest and second highest score were within 20%, cells were deemed hybrids and excluded from further analysis. We further confirmed successful cell type identification by assessing homogeneity and separation of clusters in UMAP plots, and by examining expression of top marker genes across cell types. While cell type identification with BRETIGEA package's cell type markers was comparable to the original paper's identification, we found the original paper's cell types more comprehensive as it distinguished excitatory from inhibitory neurons. Thus, we used the original paper's cell type labels for the further analysis (Supplementary Table 1). Due to low cell counts, we did not analyze pericytes and endothelial cells. The final Seurat object contained 17,723 genes and 62,741 cells.

Entorhinal Cortex

We acquired a filtered raw expression matrix of 10,850 genes and 13,214 cells, which was originally composed of 33,694 genes and 14,876 cells and filtered as described by Grubman and colleagues. A Seurat object was created and consisted of genes in at least 3 cells, and cells with at least 200 genes. Normalization was performed using Seurat's SCTransform[73] method, and Seurat's integration workflow was performed to correct the confounded batches introduced by the original study's experimental design.

Dimensionality reduction was performed using values from the integrated assay to assess successful batch correction (Supplementary Figure 1). Using the method for cell type identification described for the former cohort, we identified astrocytes, endothelial cells, neurons, microglia, oligodendrocytes, and oligodendrocyte progenitor cells. We further confirmed successful cell type identification by assessing homogeneity and separation of clusters in UMAP plots. Due to limitations in the number of cells, we excluded endothelial cells from further analyses. The final Seurat object contained 10,846 genes and 11,284 cells (Supplementary Table 2).

Cell Type-Specific Sex-stratified Differential Expression Analysis

To generate molecular signatures relative to sex in each cell type, we used the Limma[74,75] package's Voom[76] pipeline for RNA-seq. For the prefrontal and entorhinal cortices, we performed a sex-stratified analysis including *APOE* genotype as a covariate. For the entorhinal cortex cohort, while we integrated batches in our pre-processing, we were not able to include batch as a covariate, as its collinearity did not allow for an appropriate model fit.

After the design formulas were established, the DGEList object was created from a matrix of counts extracted from the corresponding Seurat objects. To improve the accuracy of mean-variance trend modeling and lower the severity of multiple testing correction, lowly expressed genes were filtered out using edgeR's FilterByExpr function with default parameters. Normalization was performed with Trimmed Mean of M-values with singleton pairing (TMMwsp), followed by voom, model fitting with a contrast matrix of each defined case-control comparison, and Empirical Bayes fitting of standard errors. We determined differentially expressed genes as those with a Benjamini-Hochberg corrected p-value less than 0.05, and an absolute LFC greater than 0.25.

Pathway Analysis

We performed an overrepresentation analysis of DEGs from the cell type-specific sex-stratified analysis of cells from the prefrontal and entorhinal cortex using g:Profiler[50], a web tool that performs functional enrichment analysis from a given gene list. We queried differentially expressed genes comparison split by upregulated and down-regulated expression and selected enriched pathways with a Benjamini-Hochberg adjusted p-value cutoff of 0.05. In addition to Gene Ontology cellular components, biological processes, and molecular functions, our enrichment analysis also provided pathways from the Human Protein Atlas, Human Phenotype Ontology, KEGG, Reactome, and Wiki pathways.

Network Visualization of Enrichment Results

We followed a previously established protocol[51] for network enrichment analysis on pathway results derived from our cell type-specific DEGs. Briefly, pathway results were imported into the Cytoscape visualization application, EnrichmentMap. Then, redundant and related pathways were collapsed into single biological themes using the AutoAnnotate Cytoscape application.

Acknowledgements

Special thanks to Dr. Katharine Yu, Dr. Idit Kosti, Dr. Dmitry Rychkov, and the rest of the Sirota lab for scientific guidance and support in this project. This work is funded by the National Institute on Aging (NIA) grants R01AG060393 and R01AG057683. This material is based upon work supported by the National Science Foundation Graduate Research Fellowship Program under Grant No. 1650113. Any opinions, findings, and conclusions or recommendations expressed in this material are those of the author(s) and do not necessarily reflect the views of the National Science Foundation or the National Institutes of Health.

Author Contributions

SB, YL, and MS conceived the study. SB performed data analysis and interpretation of results (data wrangling and pre-processing, cell type-identification, batch correction, snRNAseq differential gene expression analysis, and pathway functional enrichment), generated and compiled figures, and drafted the manuscript. YL generated figures and interpretated results for the enriched pathway network analysis and drafted the manuscript. DB assisted in developing methods and figures for the analysis and drafted the manuscript. AAR assisted in developing methods for data analysis. CWS, AT, GF, TO, and DD contributed to the discussion of methods and results as well as the implications of the findings. MS oversaw the study. All authors read and contributed to the final manuscript. The funders had no role in the design, implementation, or preparation of this manuscript.

Competing Interests

MS is on the advisory board of twoXAR. Other authors declare no competing financial interests.

References

1. Masters, C. L. *et al.* Alzheimer's disease. *Nature Reviews Disease Primers* **1**, 1–18 (2015).
2. Murray, M. E. *et al.* Neuropathologically defined subtypes of Alzheimer's disease with distinct clinical characteristics: a retrospective study. *Lancet Neurol* **10**, 785–796 (2011).
3. Scheltens, P. *et al.* Alzheimer's disease. *Lancet* **388**, 505–517 (2016).
4. Prince, M. J., Comas-Herrera, A., Knapp, M., Guerchet, M. M. & Karagiannidou, M. World Alzheimer Report 2016 - Improving healthcare for people living with dementia: Coverage, quality and costs now and in the future. (2016).
5. Bureau, U. C. An Aging World: 2015. *The United States Census Bureau* https://www.census.gov/library/publications/2016/demo/P95-16-1.html.
6. Plassman, B. L. *et al.* Prevalence of dementia in the United States: the aging, demographics, and memory study. *Neuroepidemiology* **29**, 125–132 (2007).
7. Hebert, L. E., Weuve, J., Scherr, P. A. & Evans, D. A. Alzheimer disease in the United States (2010-2050) estimated using the 2010 census. *Neurology* **80**, 1778–1783 (2013).
8. Goedert, M. & Spillantini, M. G. A century of Alzheimer's disease. *Science* **314**, 777–781 (2006).
9. Karch, C. M. & Goate, A. M. Alzheimer's disease risk genes and mechanisms of disease pathogenesis. *Biological Psychiatry* **77**, 43–51 (2015).
10. Bloom, G. S. Amyloid-β and tau: the trigger and bullet in Alzheimer disease pathogenesis. *JAMA Neurol* **71**, 505–508 (2014).
11. Busche, M. A. & Hyman, B. T. Synergy between amyloid-β and tau in Alzheimer's disease. *Nat Neurosci* **23**, 1183–1193 (2020).
12. Heneka, M. T. *et al.* Neuroinflammation in Alzheimer's disease. *Lancet Neurol* **14**, 388–405 (2015).

13. Hebert, L. E. *et al.* Change in risk of Alzheimer disease over time. *Neurology* **75**, 786–791 (2010).
14. Xu, Y. *et al.* Neurotransmitter receptors and cognitive dysfunction in Alzheimer's disease and Parkinson's disease. *Prog Neurobiol* **97**, 1–13 (2012).
15. de la Monte, S. M. & Tong, M. Brain metabolic dysfunction at the core of Alzheimer's disease. *Biochem Pharmacol* **88**, 548–559 (2014).
16. Donev, R., Kolev, M., Millet, B. & Thome, J. Neuronal death in Alzheimer's disease and therapeutic opportunities. *J Cell Mol Med* **13**, 4329–4348 (2009).
17. Dubal, D. B. Sex difference in Alzheimer's disease: An updated, balanced and emerging perspective on differing vulnerabilities. *Handb Clin Neurol* **175**, 261–273 (2020).
18. Mielke, M. M., Vemuri, P. & Rocca, W. A. Clinical epidemiology of Alzheimer's disease: assessing sex and gender differences. *Clin Epidemiol* **6**, 37–48 (2014).
19. Medeiros, A. de M. & Silva, R. H. Sex Differences in Alzheimer's Disease: Where Do We Stand? *J Alzheimers Dis* **67**, 35–60 (2019).
20. Davis, E. J. *et al.* A second X chromosome contributes to resilience in a mouse model of Alzheimer's disease. *Sci Transl Med* **12**, (2020).
21. Barnes, L. L. *et al.* Sex Differences in the Clinical Manifestations of Alzheimer Disease Pathology. *Archives of General Psychiatry* **62**, 685–691 (2005).
22. Oveisgharan, S. *et al.* Sex differences in Alzheimer's disease and common neuropathologies of aging. *Acta Neuropathol* **136**, 887–900 (2018).
23. Hohman, T. J. *et al.* Sex-Specific Association of Apolipoprotein E With Cerebrospinal Fluid Levels of Tau. *JAMA Neurol* **75**, 989–998 (2018).
24. Guerreiro, R. J., Gustafson, D. R. & Hardy, J. The genetic architecture of Alzheimer's disease: beyond APP, PSENs and APOE. *Neurobiol Aging* **33**, 437–456 (2012).

25. Altmann, A., Tian, L., Henderson, V. W., Greicius, M. D. & Alzheimer's Disease Neuroimaging Initiative Investigators. Sex modifies the APOE-related risk of developing Alzheimer disease. *Ann Neurol* **75**, 563–573 (2014).
26. Barron, A. M. & Pike, C. J. Sex hormones, aging, and Alzheimer's disease. *Front Biosci (Elite Ed)* **4**, 976–997 (2012).
27. Ibanez, C. *et al.* Systemic progesterone administration results in a partial reversal of the age-associated decline in CNS remyelination following toxin-induced demyelination in male rats. *Neuropathol Appl Neurobiol* **30**, 80–89 (2004).
28. Ghoumari, A. M., Baulieu, E. E. & Schumacher, M. Progesterone increases oligodendroglial cell proliferation in rat cerebellar slice cultures. *Neuroscience* **135**, 47–58 (2005).
29. Lasselin, J., Lekander, M., Axelsson, J. & Karshikoff, B. Sex differences in how inflammation affects behavior: What we can learn from experimental inflammatory models in humans. *Frontiers in Neuroendocrinology* **50**, 91–106 (2018).
30. Quintero, O. L., Amador-Patarroyo, M. J., Montoya-Ortiz, G., Rojas-Villarraga, A. & Anaya, J.-M. Autoimmune disease and gender: Plausible mechanisms for the female predominance of autoimmunity. *Journal of Autoimmunity* **38**, J109–J119 (2012).
31. Di Florio, D. N., Sin, J., Coronado, M. J., Atwal, P. S. & Fairweather, D. Sex differences in inflammation, redox biology, mitochondria and autoimmunity. *Redox Biol* **31**, 101482 (2020).
32. Nirzhor, S. S. R., Khan, R. I. & Neelotpol, S. The Biology of Glial Cells and Their Complex Roles in Alzheimer's Disease: New Opportunities in Therapy. *Biomolecules* **8**, (2018).
33. Luchena, C., Zuazo-Ibarra, J., Alberdi, E., Matute, C. & Capetillo-Zarate, E. Contribution of Neurons and Glial Cells to Complement-Mediated Synapse Removal during Development, Aging and in Alzheimer's Disease. *Mediators of Inflammation* **2018**, e2530414 (2018).
34. Paranjpe, M. D. *et al.* Sex-Specific Cross Tissue Meta-Analysis Identifies Immune Dysregulation in Women with Alzheimer's Disease. *bioRxiv* 2020.04.24.060558 (2020) doi:10.1101/2020.04.24.060558.

35. Mathys, H. *et al.* Single-cell transcriptomic analysis of Alzheimer's disease. *Nature* **570**, 332–337 (2019).
36. Grubman, A. *et al.* A single-cell atlas of entorhinal cortex from individuals with Alzheimer's disease reveals cell-type-specific gene expression regulation. *Nat Neurosci* **22**, 2087–2097 (2019).
37. Mirra, S. S. *et al.* The Consortium to Establish a Registry for Alzheimer's Disease (CERAD). Part II. Standardization of the neuropathologic assessment of Alzheimer's disease. *Neurology* **41**, 479–486 (1991).
38. Fernandez-Enright, F. & Andrews, J. L. Lingo-1: a novel target in therapy for Alzheimer's disease? *Neural Regen Res* **11**, 88–89 (2016).
39. Mi, S. *et al.* LINGO-1 negatively regulates myelination by oligodendrocytes. *Nature Neuroscience* **8**, 745–751 (2005).
40. Iwama, K. *et al.* A novel mutation in SLC1A3 causes episodic ataxia. *J Hum Genet* **63**, 207–211 (2018).
41. Mahmud, F. J. *et al.* Osteopontin/secreted phosphoprotein-1 behaves as a molecular brake regulating the neuroinflammatory response to chronic viral infection. *J Neuroinflammation* **17**, 273 (2020).
42. Mozhui, K. *et al.* Genetic regulation of Nrnx1 expression: an integrative cross-species analysis of schizophrenia candidate genes. *Transl Psychiatry* **1**, e25 (2011).
43. Cario, H. *et al.* Dihydrofolate Reductase Deficiency Due to a Homozygous DHFR Mutation Causes Megaloblastic Anemia and Cerebral Folate Deficiency Leading to Severe Neurologic Disease. *The American Journal of Human Genetics* **88**, 226–231 (2011).
44. Sahin, P., McCaig, C., Jeevahan, J., Murray, J. T. & Hainsworth, A. H. The cell survival kinase SGK1 and its targets FOXO3a and NDRG1 in aged human brain. *Neuropathology and Applied Neurobiology* **39**, 623–633 (2013).

45. Wang, B.-J. *et al.* ErbB2 regulates autophagic flux to modulate the proteostasis of APP-CTFs in Alzheimer's disease. *PNAS* **114**, E3129–E3138 (2017).
46. Kok, E. H. *et al.* CLU, CR1 and PICALM genes associate with Alzheimer's-related senile plaques. *Alzheimer's Research & Therapy* **3**, 12 (2011).
47. Muraoka, S. *et al.* Proteomic Profiling of Extracellular Vesicles Derived from Cerebrospinal Fluid of Alzheimer's Disease Patients: A Pilot Study. *Cells* **9**, (2020).
48. Raghavan, N. S. *et al.* Association Between Common Variants in *RBFOX1* , an RNA-Binding Protein, and Brain Amyloidosis in Early and Preclinical Alzheimer Disease. *JAMA Neurol* **77**, 1288 (2020).
49. Hua, Y., Zhao, H., Lu, X., Kong, Y. & Jin, H. Meta-Analysis of the Cystatin C(CST3) Gene G73A Polymorphism and Susceptibility to Alzheimer's Disease. *International Journal of Neuroscience* **122**, 431–438 (2012).
50. Raudvere, U. *et al.* g:Profiler: a web server for functional enrichment analysis and conversions of gene lists (2019 update). *Nucleic Acids Res* **47**, W191–W198 (2019).
51. Reimand, J. *et al.* Pathway enrichment analysis and visualization of omics data using g:Profiler, GSEA, Cytoscape and EnrichmentMap. *Nature Protocols* **14**, 482–517 (2019).
52. Chen, H., Chung, S. & Sukumar, S. HOXA5-Induced Apoptosis in Breast Cancer Cells Is Mediated by Caspases 2 and 8. *Mol. Cell. Biol.* **24**, 924 (2004).
53. Smith, R. G. *et al.* Elevated DNA methylation across a 48-kb region spanning the HOXA gene cluster is associated with Alzheimer's disease neuropathology. *Alzheimer's & Dementia* **14**, 1580–1588 (2018).
54. Kapatos, G. The neurobiology of tetrahydrobiopterin biosynthesis: A model for regulation of GTP cyclohydrolase I gene transcription within nigrostriatal dopamine neurons. *IUBMB Life* **65**, 323–333 (2013).

55. Frank, J. W., Seo, H., Burghardt, R. C., Bayless, K. J. & Johnson, G. A. ITGAV (alpha v integrins) bind SPP1 (osteopontin) to support trophoblast cell adhesion. *Reproduction* **153**, 695–706 (2017).
56. Sun, G., Cui, Q. & Shi, Y. Chapter Nine - Nuclear Receptor TLX in Development and Diseases. in *Current Topics in Developmental Biology* (eds. Forrest, D. & Tsai, S.) vol. 125 257–273 (Academic Press, 2017).
57. Davenne, M. *et al.* Hoxa2 and Hoxb2 control dorsoventral patterns of neuronal development in the rostral hindbrain. *Neuron* **22**, 677–691 (1999).
58. Hansen, D. V., Hanson, J. E. & Sheng, M. Microglia in Alzheimer's disease. *J Cell Biol* **217**, 459–472 (2018).
59. Tibbo, A. J. & Baillie, G. S. Phosphodiesterase 4B: Master Regulator of Brain Signaling. *Cells* **9**, 1254 (2020).
60. Yun, H.-Y., Dawson, V. & Dawson, T. Nitric oxide in health and disease of the nervous system. *Nitric oxide in the nervous system* 12.
61. Miao Robert Q. *et al.* Dominant-Negative Hsp90 Reduces VEGF-Stimulated Nitric Oxide Release and Migration in Endothelial Cells. *Arteriosclerosis, Thrombosis, and Vascular Biology* **28**, 105–111 (2008).
62. Guo, Y. *et al.* MicroRNAs in Microglia: How do MicroRNAs Affect Activation, Inflammation, Polarization of Microglia and Mediate the Interaction Between Microglia and Glioma? *Front. Mol. Neurosci.* **12**, (2019).
63. Theotokis, P. *et al.* Nogo receptor complex expression dynamics in the inflammatory foci of central nervous system experimental autoimmune demyelination. *Journal of Neuroinflammation* **13**, 265 (2016).
64. Whitsett, J. *et al.* Endothelial cell superoxide anion radical generation is not dependent on endothelial nitric oxide synthase-serine 1179 phosphorylation and endothelial nitric oxide synthase dimer/monomer distribution. *Free Radic Biol Med* **40**, 2056–2068 (2006).

65. Stuart, T. *et al.* Comprehensive Integration of Single-Cell Data. *Cell* **177**, 1888-1902.e21 (2019).

66. Belonwu, S. *et al. Single-cell transcriptomic analysis elucidates APOE genotype specific changes across cell types in two brain regions in Alzheimer's disease*. https://www.researchsquare.com/article/rs-291648/v1 (2021) doi:10.21203/rs.3.rs-291648/v1.

67. Buckley, R. F. *et al.* Sex Differences in the Association of Global Amyloid and Regional Tau Deposition Measured by Positron Emission Tomography in Clinically Normal Older Adults. *JAMA Neurol* **76**, 542–551 (2019).

68. R Core Team. R: A Language and Environment for Statistical Computing. https://www.r-project.org/ (2020).

69. R Studio Team. RStudio: Integrated Development Environment for R. https://rstudio.com/ (2020).

70. Ginestet, C. ggplot2: Elegant Graphics for Data Analysis. *Journal of the Royal Statistical Society: Series A (Statistics in Society)* (2011) doi:10.1111/j.1467-985x.2010.00676_9.x.

71. Conway, J. R., Lex, A. & Gehlenborg, N. UpSetR: an R package for the visualization of intersecting sets and their properties. *Bioinformatics* **33**, 2938–2940 (2017).

72. McKenzie, A. T. *et al.* Brain Cell Type Specific Gene Expression and Co-expression Network Architectures. *Scientific Reports* **8**, 1–19 (2018).

73. Hafemeister, C. & Satija, R. Normalization and variance stabilization of single-cell RNA-seq data using regularized negative binomial regression. *Genome Biology* **20**, 296 (2019).

74. Ritchie, M. E. *et al.* limma powers differential expression analyses for RNA-sequencing and microarray studies. *Nucleic Acids Res* **43**, e47 (2015).

75. Phipson, B., Lee, S., Majewski, I. J., Alexander, W. S. & Smyth, G. K. Robust hyperparameter estimation protects against hypervariable genes and improves power to detect differential expression. *Ann Appl Stat* **10**, 946–963 (2016).

76. Law, C. W., Chen, Y., Shi, W. & Smyth, G. K. voom: precision weights unlock linear model analysis tools for RNA-seq read counts. *Genome Biol* **15**, R29 (2014).

Figures

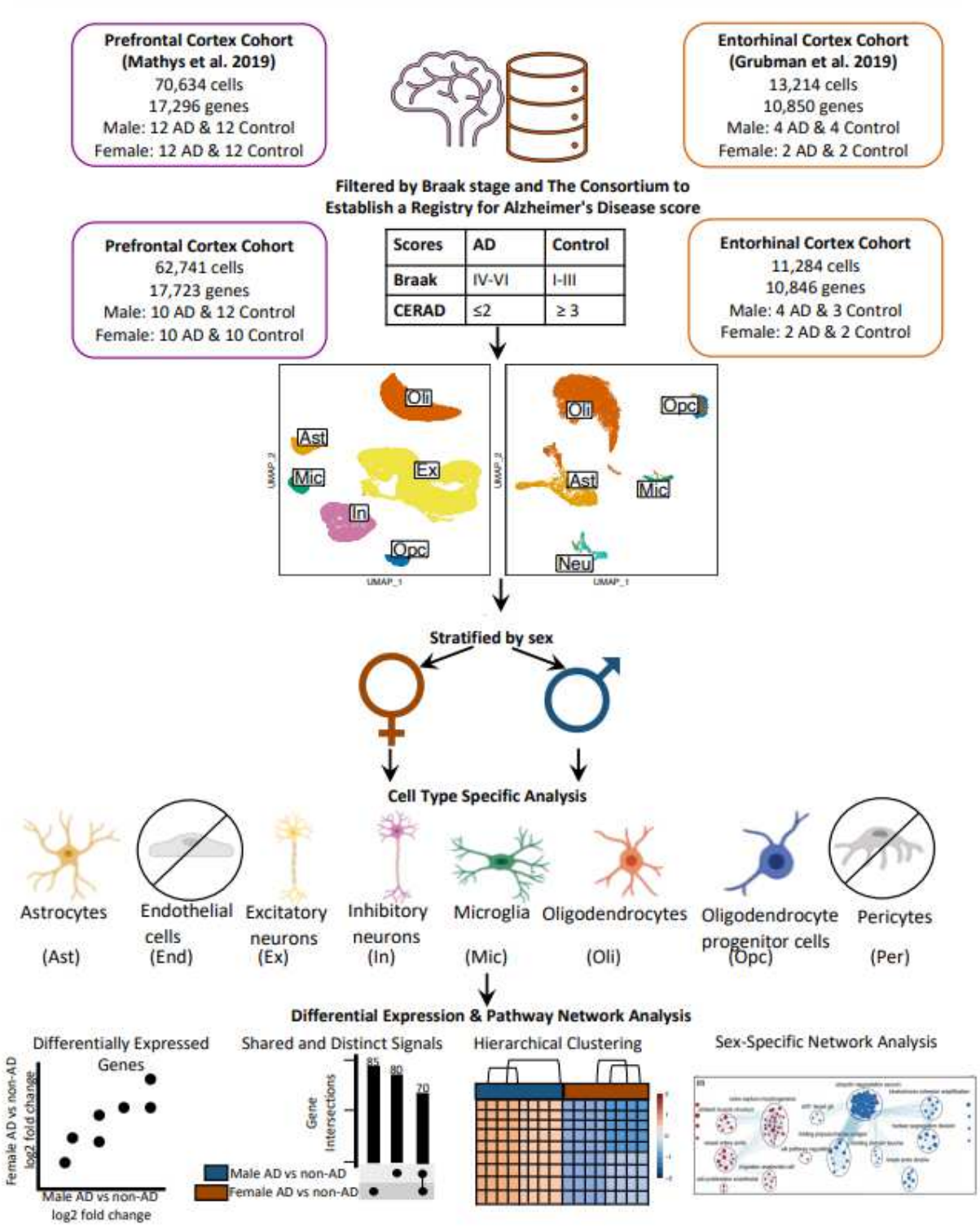

Figure 1

Overview of cohort sample definition and workflow for sex-stratified cell type-specific differential gene expression and functional enrichment. AD and non-AD cells were determined based on tau (Braak) and amyloid β plaque (CERAD) burdens. Cell types were identified, and AD versus non-AD differential

expression and pathway network enrichment analyses were performed separately for each sex in each cell type.

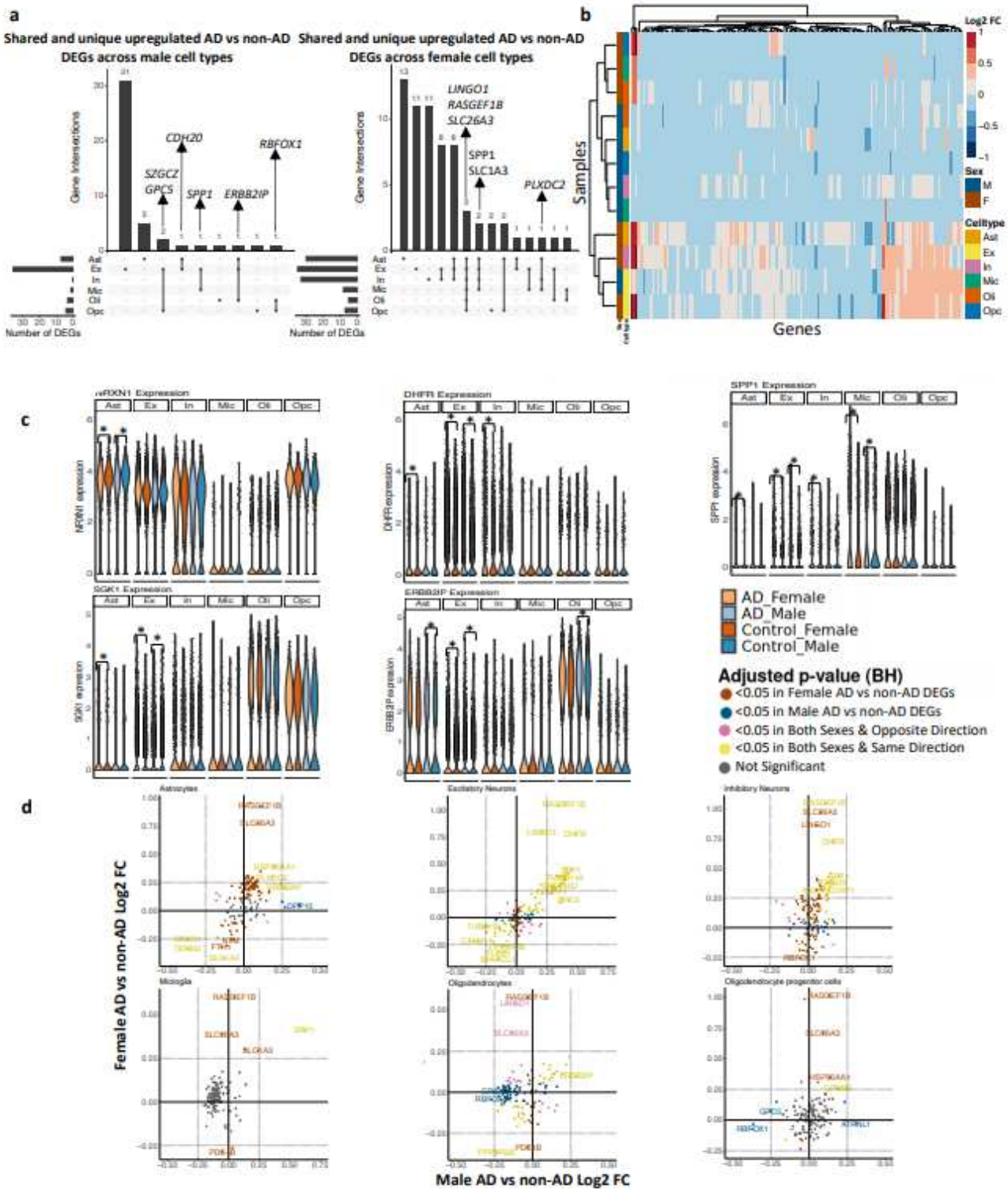

Figure 2

Sex-stratified cell type-specific differential gene expression signatures in the prefrontal cortex. a. Upset plots indicating intersections of AD versus non-AD differentially expressed genes (DEGs) (Benjamini-Hochberg (BH) adjusted p-value < 0.05 and absolute log2 fold change (FC) > 0.25) across cell types.

Rows correspond to cell types. The bar chart shows the number of single and common sets of DEGs across cell types. Single filled dots represent a unique set of DEGs for the corresponding cell type. Multiple filled black dots connected by vertical lines represent common sets of DEGs across cell types, b. log2 FC scores of all genes in the DE analysis clustered by cell type and sex, c. LINGO1, PLXDC2, SPP1, RBFOX1, ERBB21P expression. Asterisks represent meeting both significance and absolute log2 FC thresholds. Colors correspond to sex and AD status, d. Pairwise DEG plots of DEGs in male and female samples using log2 FC scores. Genes shown are significant and have a log2 FC > 0.25 in at least one sex. Colors indicate significance level of DEGs and whether DEGs are unique or shared by both sexes.

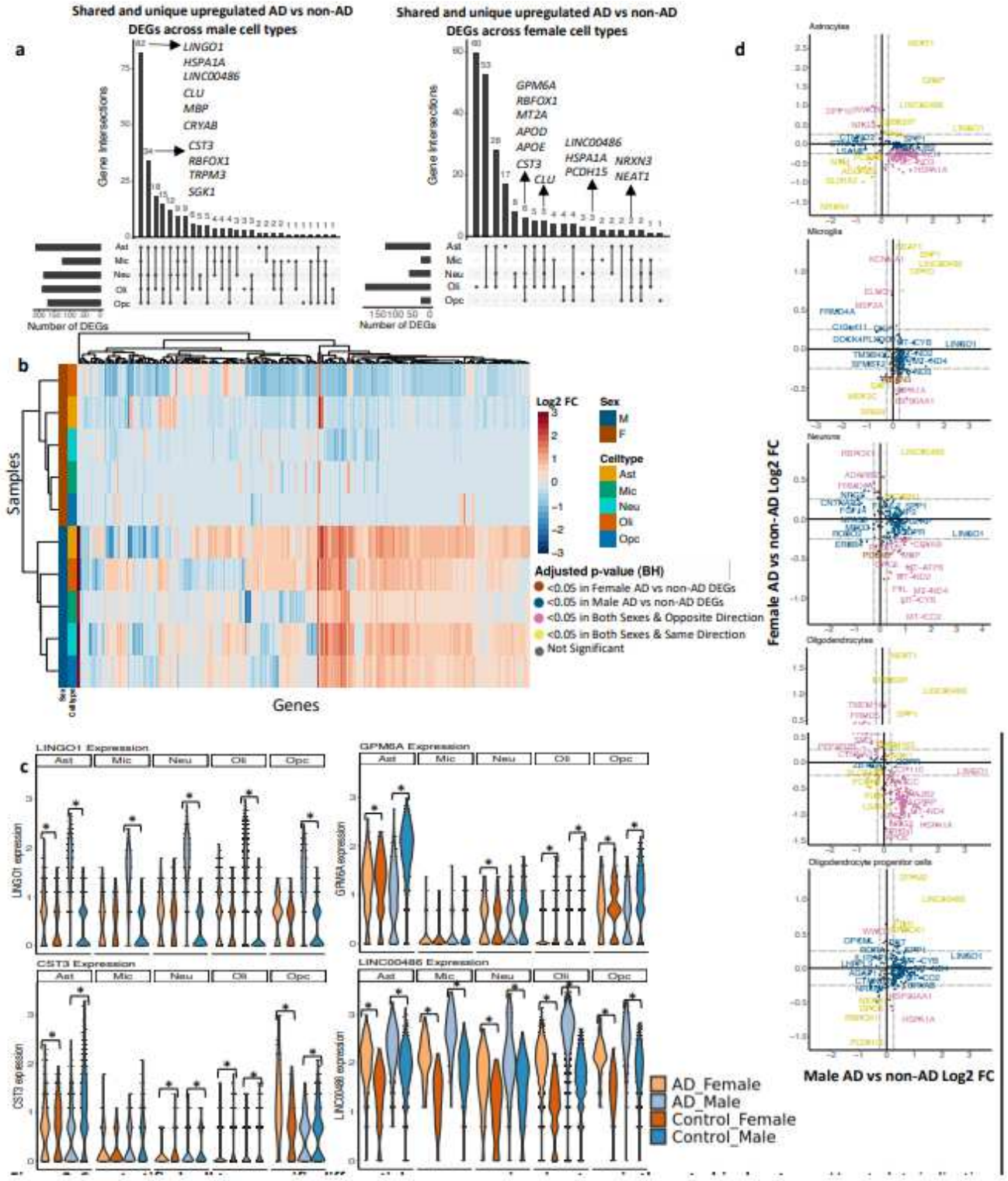

Figure 3

Sex-stratified cell type-specific differential gene expression signatures in the entorhinal cortex. a. Upset plots indicating intersections of AD versus non-AD differentially expressed genes (DEGs) (Benjamini-Hochberg (BH) adjusted p-value < 0.05 and absolute log2 fold change (FC) > 0.25) across cell types. Rows correspond to cell types. The bar chart shows the number of single and common sets of DEGs across cell types. Single filled dots represent a unique set of DEGs for the corresponding cell type.

Multiple filled black dots connected by vertical lines represent common sets of DEGs across cell types, b. log2 FC scores of all genes in the DE analysis clustered by cell type and sex, c. LINGO1, GPM6A, CST3, LINC00486 expression. Asterisks represent meeting both significance and absolute log2 FC thresholds. Colors correspond to sex and AD status, d. Pairwise DEG plots of DEGs in male and female samples using log2 FC scores. Genes shown are significant and have a log2 FC > 0.25 in at least one sex. Colors indicate significance level of DEGs and whether DEGs are unique or shared by both sexes.

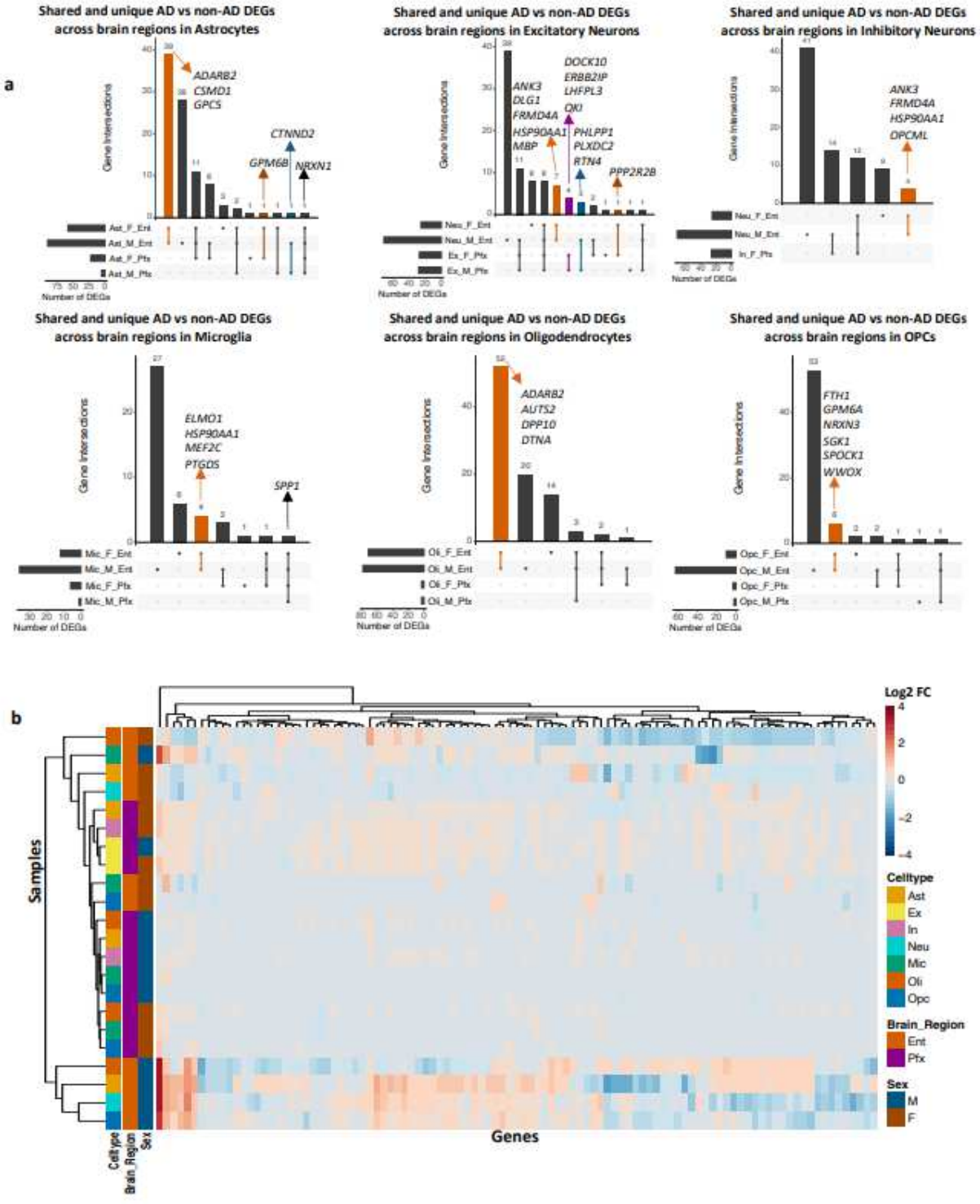

Figure 4

Sex-stratified cell type-specific disease signatures across brain regions. a. Upset plots indicating intersections of AD versus non-AD differentially expressed genes (DEGs) (Benjamini-Hochberg (BH) adjusted p-value < 0.05 and absolute log2 fold change (FC) > 0.25) within cell types across brain region and sex. Rows correspond to brain region and sex pairings. The bar chart shows the number of single and common sets of DEGs across brain regions and sex. Single filled dots represent a unique set of DEGs for the corresponding brain region and sex. Multiple filled black dots connected by vertical lines represent common sets of DEGs across brain region and sex. Bar chart colors correspond to whether DEGs are shared by brain regions or sex using the bottom right key, b. log2 FC scores of all genes in the DE analysis of both brain regions clustered by cell type, brain region, and sex.

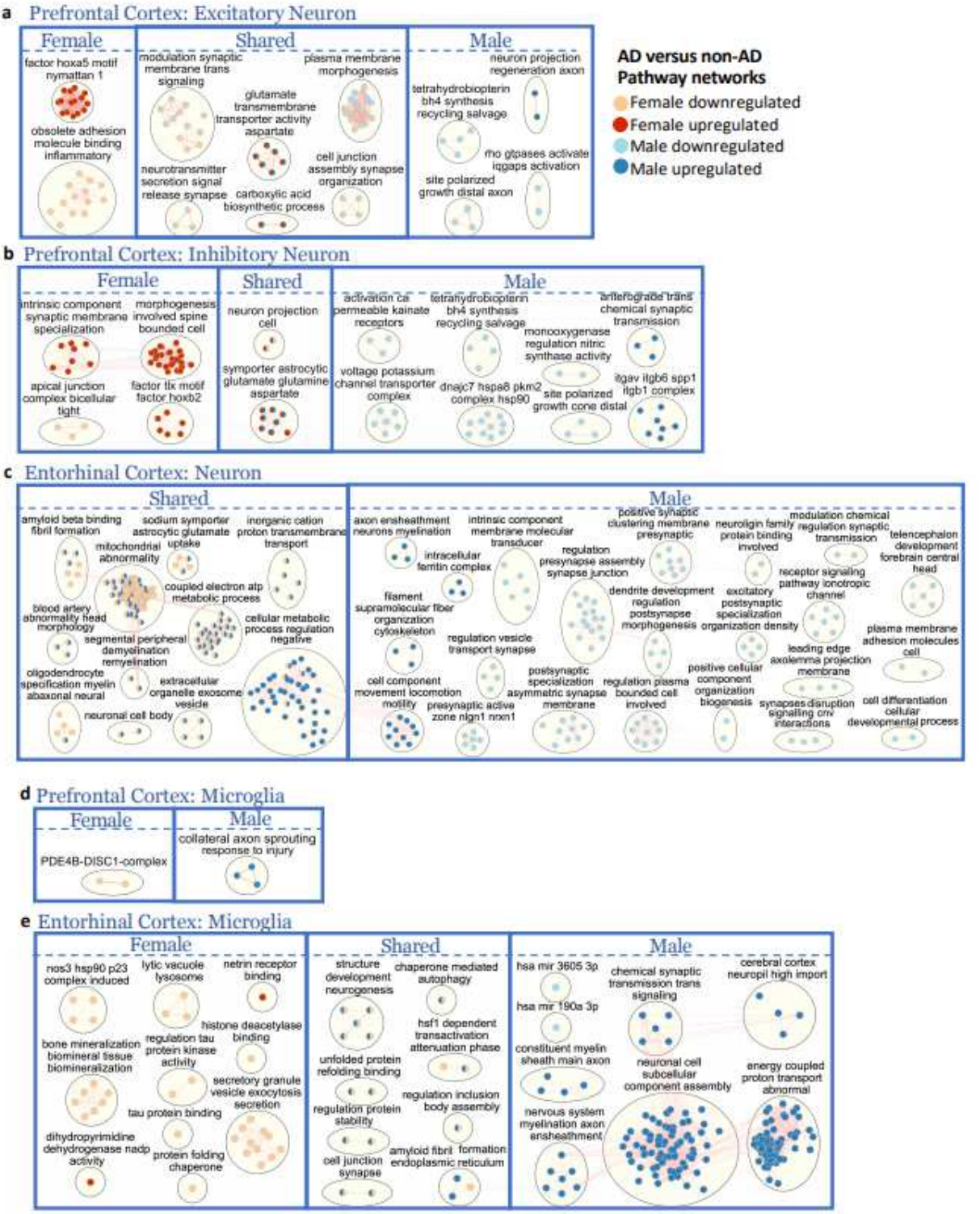

Figure 5

Enriched disease pathway networks in female and male neurons and microglia. AD compared to non-AD functionally enriched pathways with a Benjamini-Hochberg (BH) adjusted p-value < 0.05 clustered into biological themes for a. excitatory and b. inhibitory neurons from the prefrontal cortex, c. neurons from the entorhinal cortex, and microglia from the d. prefrontal, and e. entorhinal cortices. Lines represent gene set overlaps with magnitude showed by thickness.

Supplementary Files

This is a list of supplementary files associated with this preprint. Click to download.

- BelonwuLietalFigures.pdf
- Table1.txt
- Table2.txt
- Table3.txt
- Table4.txt
- SupplementaryTable1.txt
- SupplementaryTable2.txt
- SupplementaryTable3.txt
- SupplementaryTable4.txt
- SupplementaryTables58.xlsx